Internal Transport Barrier triggering by rational magnetic flux surfaces in tokamaks

E. Joffrin 1), C.D. Challis 2), G.D. Conway 3), X. Garbet 1), A. Gude 3), S. Guenther 3), N. C. Hawkes 2), T.C. Hender2), D. Howell 2), G.T.A. Huysmans 1), E. Lazzaro 4), P. Maget 1), M. Marachek 3), A.G. Peeters 3), S.D. Pinches 3), S. Sharapov 2), and the JET-EFDA contributors*

1) Association Euratom-CEA , Cadarache, F-13108, France.
2) Euratom/UKAEA Fusion Association, Culham Science Centre, Abingdon, Oxfordshire, OX14 3DB, UK.
3) Max-Planck-Institut fur Plasmaphysik, Euratom Association, 85748, Garching Germany.
4) Istituto di Fisica del Plasma del CNR, Assoc. Euratom-ENEA-CNR per la Fusione, 20125 Milan Italy.

E-mail address of main author: ejoffrin@jet.uk

Abstract: The formation of Internal Transport Barriers (ITBs) has been experimentally associated with the presence of rational q-surfaces in both JET and ASDEX Upgrade. The triggering mechanisms are related to the occurrence of magneto-hydrodynamic (MHD) instabilities such as mode coupling or fishbone activity. These events could locally modify the poloidal velocity and increase transiently the shearing rate to values comparable to the linear growth rate of ITG modes. For JET reversed magnetic shear scenarios, ITB emergence occurs preferentially when the minimum q reaches an integer value. In this case, transport effects localised in the vicinity of zero magnetic shear and close to rational q values may also contribute to the formation of ITBs.The role of rational q surfaces on ITB triggering stresses the importance of q profile control for advanced tokamak scenario and could contribute to lower substantially the access power to these scenarios in next step facilities.

1. Introduction

Recently, it was identified in JET [1] and ASDEX Upgrade [2] that rational q-surfaces and in particular low order q rational are playing a key role in the internal transport barrier (ITB) formation for both reversed and low positive magnetic shear. The variety of q-profile is usually obtained in the plasma current ramp-up using various combination of heating schemes. In JET, for example, low positive shear target profiles are produced without any heating or with small level of Ion Cyclotron Resonance Heating (ICRH) power. Strong reversed magnetic shear profiles are created by pre-heating the plasma with Lower Hybrid Current Drive (LHCD). The combined effect of off-axis current drive and electron heating by the lower hybrid wave can result in very large value of the central safety factor q_o. This tailoring of the target current profile has made possible the study of the ITB triggering mechanism for different value of the magnetic shear in the plasma centre.

This paper first summarises the experimental evidence showing the relation between rational surfaces and ITB emergence. The role of MHD events taking place on these integer q-surfaces is presented for ASDEX Upgrade and low positive magnetic shear in JET. In the fourth section, an explanation for the creation of ITB in reversed magnetic shear at q_{min}=2 or 3 is also put forward on the basis of the recent theoretical works on rational surface rarefaction.

2. Relation between rational surface and internal transport barrier formation

Several independent experimental studies in JET and ASDEX Upgrade have confirmed that rational surface are at the origin of the internal transport barrier for both low positive and strongly reversed shear. In ASDEX Upgrade, the emergence of ITB in reversed magnetic shear has been related to the presence of fishbone on the q=2 surface [2]. In JET, internal transport barriers have been observed in correlation with integer q surface such as q=1, 2 or 3 for low positive shear discharges [1]. More recent experiments have extended this

* *see annex of J. Pamela et al., Fusion Energy 2002 (Proc 19th IAEA, Lyon, 2002), Iaea, Vienna.*

analysis to reversed shear target q profile [3]. Figure 1a shows the effect of the main heating power (NBI + ICRH) on the ITB formation. As the power increases, the emergence of the ITB determined by the JET ITB criterion [4] is delayed. The determination of q profiles from motional Stark effect and infrared polarimetry shows that this emergence time coincides with the time when q_{min} reaches 2 (fig 1b). The fact that the ITB is triggered when q_{min} reaches 2, confirms that the access to the ITB regime is not clearly linked to the input power, but rather to an optimum q profile when the main heating is applied.

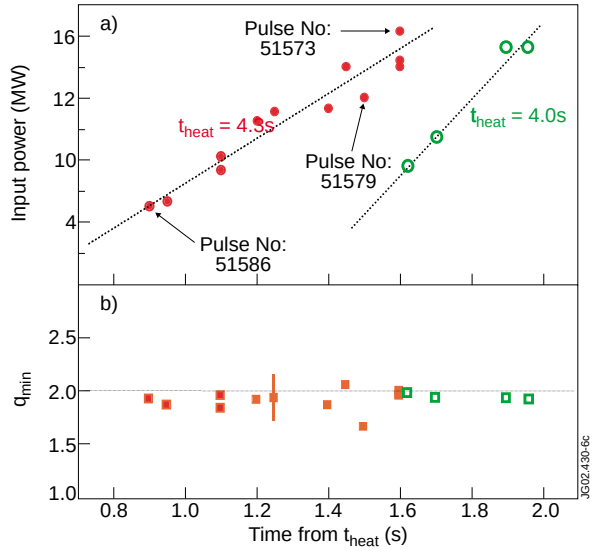

Fig 1: Emergence time of the ITB in strong reversed shear. The ITB triggering does not appear to depend on the input power level a) but is correlated with q_{min} reaching the q=2 surface b). (t_{heat} is the time when the main heating is applied)

The presence of the q=2 surface at q_{min} is experimentally confirmed by the detection of n=2 to n=6 Alfvèn cascades which can only occur when the condition m-n.q_{min}(t)=0 and is fulfilled as q_{min} passes q=2 [3]. This analysis is showing that the emergence of the ITB does not depend on the input power but on the presence of integer q-surfaces close to the low or zero shear regions. The importance of rational surface stresses the role of the q profile in the ITB formation and the need for q profile control for advanced tokamak operation.

3. ITB Trigger mechanisms in ASDEX Upgrade

Recent observations [2] have indicated that the formation of internal transport barriers in ASDEX Upgrade are preceded by fishbone activity on q-surfaces such as q=2, i.e. oscillation of the internal kink driven by the fast ion population. The mechanism by which this happens relies on the interaction between these fast ions with the kink distortion of the magnetic field. The time evolution of the fast ion radial current has been computed using the radial magnetic structure of the mode inferred from experimental data from the electron cyclotron emission (ECE) and magnetic diagnostics. From this radial current, the effective radial electric field is inferred and the produced sheared ExB flow deduced. A comparison of the shearing rate calculated for ASDEX Upgrade parameters indicates that fishbones with a sufficiently high repetition frequency (typically above the effective collision time scale) give shearing rate comparable with estimates of the linear growth rate of ion temperature modes (ITG) modes. Fishbones are thus a suitable candidate for the triggering of ITBs.

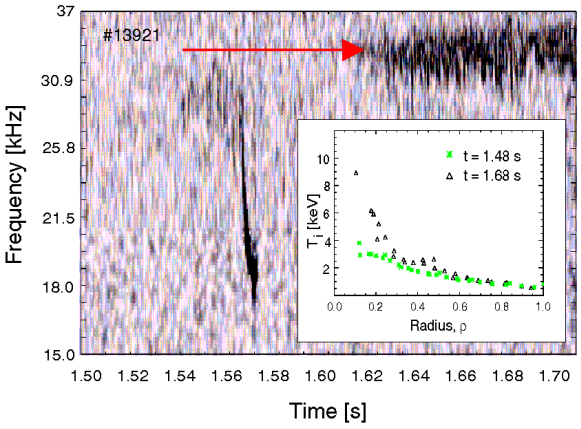

Fig 7: Fishbone activity (arrow) at the ITB emergence in ASDEX Upgrade.

4. Trigger mechanism in low positive magnetic shear in JET.

In JET, a recent experimental study has shown that the ITB emergence is well correlated with an external kink mode is destabilised as an integer q surface (q=4, q=5 or q=6)

enters the plasma in the current ramp-up [1]. Since ITBs are formed in the vicinity of internal integer q surfaces, toroidal mode coupling has been put forward as the most plausible candidate mechanism to explain the link between the edge MHD occurrence and the ITB emergence time. Simulations with the CASTOR code have confirmed that strong mode coupling can occur between the edge MHD mode and the internal q surface. The destabilisation of the MHD at q=2 or q=3 by the coupling process could provide a locally enhanced sheared flow by 'mode braking', and act as a trigger for the ITB formation.

To examine this hypothesis and evaluate the effect of mode braking on plasma flow, the model shown below make use of the linearised MHD equations including toroidal effect between two resonant layers. The resonance layers are supposed to be in the non-linear regime and the plasma response is determined by diamagnetism and transverse transport (diffusion and viscosity). These equations are solved together with the evolution equations for the plasma flow in both toroidal and poloidal directions.

The system of coupled equations between the poloidal and toroidal rotation and the growth rates (or Δ') of the edge and internal modes is calculated from the variational principle for a given n number (here n=1). The coupled equation for the evolution of the normalised island width W and phase ϕ are expressed for each resonant surface as [5]:

$$R_b \frac{\partial W_b}{\partial t} = \Delta'_b + \frac{C}{s_b}.\frac{W_e^2}{W_b^2}.\cos(\phi_e - \phi_b) \qquad \text{and} \qquad R_e \frac{\partial W_e}{\partial t} = \Delta'_e + C.s_b.\frac{W_b^2}{W_e^2}.\cos(\phi_e - \phi_b)$$

$$\frac{\partial \phi_b}{\partial t} = k_\theta.V_b^* + k_\theta.V_{\theta b} + k_\varphi.V_{\varphi b} + \frac{C}{\kappa_b.s_b}.W_e{}^2.W_b.\sin(\phi_e - \phi_b)$$

$$\text{and} \quad \frac{\partial \phi_e}{\partial t} = k_\theta.V_e^* + k_\theta.V_{\theta e} + k_\varphi.V_{\varphi e} - \frac{C.s_b}{\kappa_e}.W_b^2.W_e.\sin(\phi_e - \phi_b)$$

In these equations, the index "b" denotes the quantities at the barrier location and "e" at the edge. C is the coupling parameter and is approximated by C~a/R. R_b , R_e and s_b , s_e are respectively the resistive times and the magnetic shears at each resonant surface. Finally κ_b (and κ_e) are given in [6]: $\kappa_b = 88.D.\beta.\left(\frac{qR}{s_b.a}\right)^2.\frac{1}{k_\theta^2.a}.c_s$, using the Gyro-Bohm approximation for the diffusion coefficient D and where c_s is the sound speed. The equation of motion for the plasma in the toroidal and poloidal direction at the location of the rational surface are described by:

$$m.n.\frac{\partial V_\theta}{\partial t} = P_\theta - m.n.\nu_{neo}(V_\theta - k_{neo}V^*) \qquad \text{and} \qquad m.n.\frac{\partial V_\varphi}{\partial t} = P_\varphi + m.n.\frac{1}{r}.\frac{d}{dr}\left(r\mu\frac{dV_\varphi}{dr}\right) + P_{beam}$$

$V^* = \frac{2T_i}{e.a.B_o}$, $\nu_{neo} = \nu_{ii}.q^2.(R/a)^{3/2}$, μ the viscosity and k_{neo}~1.17 in the collisionless regime. P_θ and P_φ are the poloidal and toroidal momentum per unit volume transferred to the plasma by the mode on the considered resonance layers. This momentum will act on the plasma over a spatial range determined by a form factor L such that $\int L(\rho).d\rho = 1$ where ρ=r/a is the normalised radius. This function L depends on the model employed outside the island separatrix. In the present calculation, the behaviour of the flow shear away from the separatrix of the island is described as in reference [7] taking into accound the diamagnetic effect in the vicinity of the island. In this case, the function L is decribed by an exponential and the typical width of the region where the plasma is entrained by the island is estimated to be: $\lambda = \rho_s.\sqrt{\frac{\mu}{D}}$, where ρ_s is the ion larmor radius.

In steady state and without mode coupling, one can note from the above equations that the plasma at the rational surface will rotate with the diamagnetic frequency in the poloidal direction and with the neutral beam momentum P_{beam} in the toroidal direction.

These equations are solved using, the q=2 surface is as the internal surface and the external surface q=4 is artificially destabilised by an increase of its Δ_e'. This choice reproduces the observed experimental situation where the external mode on the q=4 surface is destabilised by an excess of edge current and couples with the q=2 surface at the ITB location. Figure 3 shows the behaviour of the simulated poloidal and toroidal velocity using typical plasma parameters (T_e=2keV, B_T=2.6T, n_e=2.10^{19} m^{-3}). The edge pertubation is simulated by an increase of Δ_e' from 0 to 2, corresponding to an edge perturbation $\tilde{B}_\theta / B_\theta \approx 10^{-3}$. The poloidal velocity starts to oscillate with an amplitude of about 400m/s. This oscillation indicates that the two resonant surfaces are not locked to each other but are in an intermediate state where the edge mode starts to brake the growing q=2 island. The change in toroidal rotation is relatively modest and the island at the q=2 surface increases to a size of less than 2cm. This is making difficult the detection of this island by magnetic measurements on the wall of the vacuum vessel. However, the effective change of poloidal rotation (~200m/s) imposed by the q=2 island will strongly modify the shear flow outside the island separatrix. Using the cylindrical definition of Hahm and Burrell [8], the shear rate is defined for the case of low magnetic shear and sharp electric field gradients:

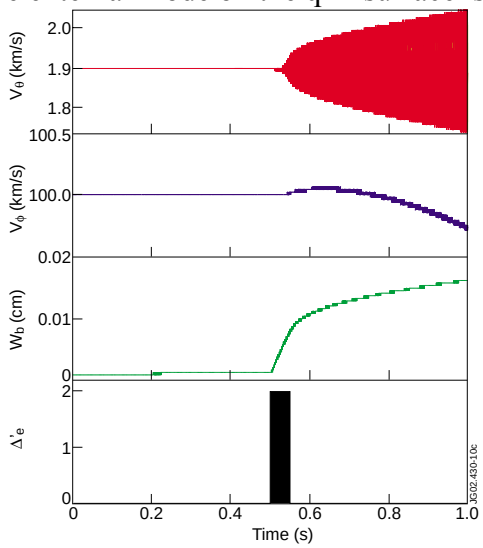

Fig 3; Simulation of the poloidal and toroidal flow at the q=2 surface when an edge perturbation grows at the q=4 surface at the edge.

$$\gamma_E \approx \left| \frac{d}{dr}\left(\frac{E_r}{B_o}\right) \right| \approx \left| \frac{d}{dr} V_\theta \right| \approx \frac{V_\theta}{\lambda} \approx 5.10^4\, s^{-1} \quad \text{and} \quad \frac{\gamma_{lin}}{k_\theta . \rho_s} = \frac{V_{th}}{\sqrt{a.R}} = 2.210^5\, s^{-1}$$

showing that mode braking is capable of triggering an ITB by inducing strong local shearing rate exceeding the linear growth rate of ITG turbulence (γ_{lin}) for $k_\theta.\rho_s$ of the order of 0.2.

4. Trigger mechanism in reversed magnetic shear in JET.

In reversed shear q profile the emergence of ITBs has also been confirmed to correlated with s=0 reaching a rational magnetic q-surface such as 2 or 3 as explained in section 1. Figure 4a shows the evolution of the temperature gradient as the zero shear point reaches the rational surface q=2. From this point, two internal transport barriers develop at two different radial locations: one in the negative shear and the other in the positive shear region. This behaviour looks quite systematic and has been described in more details in reference [3]. It cannot be explained only by the velocity shear argument. This would be indeed coincidental to see the strong shear flow propagating in two different directions radially. In addition, no MHD activity has been in general observed at the time of the ITB formation in contrast to the low positive shear case.

On the other hand, the argument of the rarefaction of flux surfaces already put forward by previous authors [9, 10] could provide an explanation for this behaviour. In the vicinity of low order rational surface, sharp barrier could develop at the location of zero magnetic shear. The rarefaction of resonant surfaces around low order rational q can create gaps which are not balanced by an increase of the turbulence radial correlation length. The width of the gap

scales as the square root of the Larmor radius and depend on the curvature of the q profile as: $d_{gap} = \left[\frac{2.q_{min}.\rho_i}{n.r_{min}.q''_{min}} \right]^{\frac{1}{2}}$. When this gap width exceeds the turbulence correlation length L_c (scaling like ρ_i for gyro-Bohm scaling), simulations are suggesting that an internal transport barrier can be formed [10]. It should be noted that the q profile (i.e. q") is the dominant factor in d_{gap} since ρ_i scales as $T_e^{1/2}/B_o$ which is itself roughly constant with the plasma radius r.

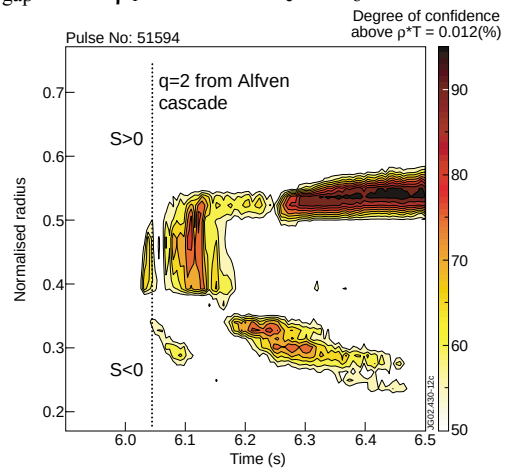

Fig 4a: ITB criterion calculated for pulse 51591. When the q_{min} reaches q=2 two ITB are created on each side of q_{min}

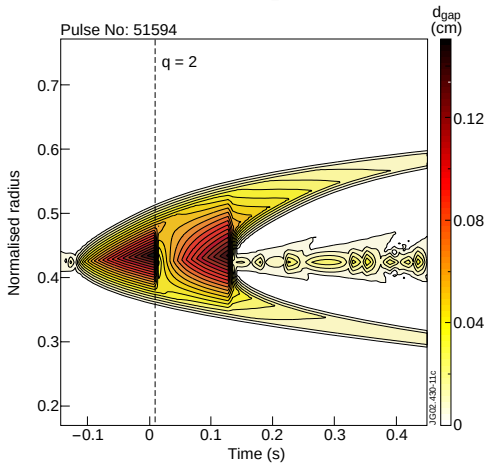

Fig 4b: Simulation of the gaps between rational surfaces up to n=m=80, as a reversed the profile is scanned across the q=2 surface.

The evolution of the gaps between resonant surfaces has been computed for pulse 51579. The experimental q profile shape is scanned across the q=2 surface and the gaps calculated for toroidal and poloidal number up to 80 (fig 4b), i.e. $k_\theta.\rho_s \sim 0.5$. When the q=2 surface is reached a large gap opens and then two gaps on each side of the q=2 surfaces propagating on each side of q_{min}. Shortly after, it appears that high n and m resonant surfaces are developing in between these two gaps, dividing them and making possible the formation of two internal transport barriers at two different radial locations as observed by the experiment. This indicates that the evolution of rational surfaces around a low integer q-surface could be at the origin of the formation of the two observed ITBs.

5. Conclusions

The analysis of ITB triggering mechanism in JET and ASDEX-Upgrade has demonstrated that the physics properties (MHD and transport) of resonant q-surfaces are essential for the understanding of ITB formation. Ultimately the knowledge and the control of the triggering conditions to form an ITB will assist in minimising the required input power to access ITB regimes in advanced tokamak plasmas for larger size devices.

References

[1] E. Joffrin et al. Nuc Fus **42** (2002) 235
[2] S. Pinches et al. 28th EPS Conference on Control. Fusion and Plasma Physics **25A** P1.008
[3] E. Joffrin et al. Plasma Physics and Controlled Fusion **44** (2002) 1739
[4] G. Tresset et al. Nuc Fus **42** (2002) 520
[5] D. Edery and A. Samain, Plasma Physics and Controlled Fusion **32** (1990) 93
[6] A. Samain, Plasma Physics and Controlled Fusion **26** (1984) 731
[7] J. W. Connor et al., Phys. Plasma **8** (2001) 2835
[8] T. S. Hahm and K.H. Burrell, Phys. Plasma **2** 1648
[9] F. Romanelli and F. Zonca, Phys. Fluids B **5** 4081
[10] X. Garbet et al, Phys. Plasma **8** (2001) 2793 and this conference TH/C2-1